

# Conjugated Polymers as Photoredox Catalysts: Visible-Light-Driven Reduction of Aryl Aldehydes by Poly(*p*-phenylene)

Miao Zhang,<sup>[a]</sup> William D. Rouch,<sup>[a]</sup> and Ryan D. McCulla<sup>\*[a]</sup>

**Keywords:** Photocatalysis / Conjugation / Polymers / Chemoselectivity / Reduction

The use of visible light in photocatalysis has been intensively studied because of its natural abundance, ease of use, and promising potential for industrial applications. However, there are several challenges to utilizing visible light for organic functional group transformations. These challenges include the low absorptivity of most organic compounds in the visible spectrum, and side reactions are often prevalent in photochemical reactions. Visible-light-sensitive catalysts offer a means to overcome these obstacles. Conjugated polymers are semiconductors that offer a large range of redox potentials, they are stable, and they often absorb visible light. Despite these desirable properties for photocatalysis, only a limited number of organic reactions utilizing conju-

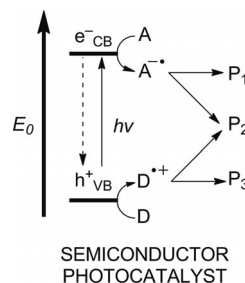
gated polymers as photocatalysts have been reported. In one such example, poly(*p*-phenylene) was used to induce the pinacol coupling reaction of benzaldehyde upon irradiation with visible light. In this work, visible light, thiols, and poly(*p*-phenylene) were employed to reduce aryl aldehydes to their respective alcohols to better characterize the reaction mechanisms of this system. The effects of varying reaction conditions on the rate of photocatalysis indicated interfacial electron transfer from the poly(*p*-phenylene) surface to the substrate as the initial productive step. Additionally, the chemoselective reduction of aryl aldehydes over aryl ketones and alkyl aldehydes was achieved with this system.

## Introduction

The use of photocatalysts in chemical synthesis has a venerable history, and recently, the conjoining of photoredox catalysts and visible light for applications in organic synthesis has become an expanding area of research.<sup>[1]</sup> Notably, organometallic ruthenium(II) and iridium(III) polypyridine complexes have been used for cycloadditions, reductive dehalogenations, enantioselective alkylations, radical additions, and C–H bond activation.<sup>[2]</sup> Additionally, small organic photosensitizers have recently been used to promote radical additions into C=C and C=O and oxidative C–C and C–P bond couplings.<sup>[3]</sup> Although the aforementioned homogeneous photoredox catalysts have proven utility, heterogeneous photocatalysts can be desirable for certain applications.

Heterogeneous photocatalysts are often semiconductors.<sup>[4]</sup> Irradiation of a semiconductor promotes electrons from the valence band to the conduction band, and the resulting charge carriers ( $h^+_{VB}$  and  $e^-_{CB}$ ) can be used to oxidize or reduce adsorbed species with the proper redox potentials (Scheme 1). To catalyze organic reactions, photocatalytic systems are designed to take advantage of the reactivity of the nascent radical-anion ( $A^{\cdot-}$ ) or radical-

cation ( $D^{\cdot+}$ ) to generate new products through unimolecular rearrangements or reactions with other species at the surface or in bulk solution. Thus, photocatalysts can be used to promote both oxidative and reductive transformations of organic substrates.



Scheme 1.

The strong oxidation potential of the  $\text{TiO}_2$  valence band (2.5 V vs. NHE) allows  $\text{TiO}_2$  to photocatalytically degrade many organic compounds, which has made the use of  $\text{TiO}_2$  as a means to remediate pollution an extremely active area of research.<sup>[5]</sup> Taking advantage of the strongly oxidative properties of  $\text{TiO}_2$  remains one of the most common applications of heterogeneous photoredox catalysts in synthetic organic reactions.<sup>[6]</sup> A variety of organic compounds such as aliphatic alcohols,<sup>[7]</sup> aromatic alcohols,<sup>[8]</sup> alkenes,<sup>[9]</sup> and hydrocarbons<sup>[10]</sup> can undergo photo-oxidation catalyzed by  $\text{TiO}_2$ . Fox and co-workers provided many synthetic and mechanistic insights into photocatalytic properties of  $\text{TiO}_2$ , including the role of electron-transfer through the detection

[a] Department of Chemistry, Saint Louis University,  
3501 Laclede Ave, 63103 St. Louis, MO, USA  
Fax: +1-314-977-2521  
E-mail: rmccull2@slu.edu  
Homepage: <http://www.slu.edu/~rmccull2/>

Supporting information for this article is available on the WWW under <http://dx.doi.org/10.1002/ejoc.201200437>.

## FULL PAPER

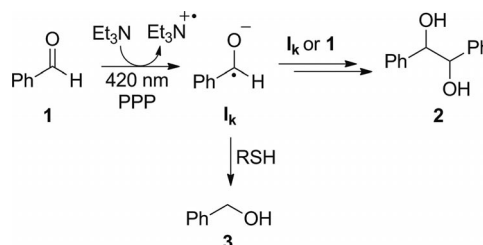
of radical cations in the *cis-trans* isomerization of stilbene.<sup>[11]</sup> They also demonstrated that the oxidation of olefins to carbonyls occurred at the semiconductor–liquid interface rather than in bulk solution.<sup>[12]</sup> Formylation of primary and secondary amines, which were frequently adopted as sacrificial electron donors, was the ultimate fate for amines in semiconductor photocatalytic systems.<sup>[13]</sup> Compared to TiO<sub>2</sub>, which only has a moderate conduction band potential (−0.5 V vs. NHE),<sup>[14]</sup> the conjugated polymer poly(*p*-phenylene) (PPP) has a much higher conduction band potential of −2.0 vs. NHE.<sup>[15]</sup> Electron transfer to an acceptor can only occur easily if the reduction potential of the acceptor is less negative than the conduction band potential of the photocatalyst. Thus, PPP is expected to be a much stronger reductive photocatalyst than TiO<sub>2</sub> and most other inorganic semiconductors.

Despite the ubiquitous application of conjugated polymers as field-effect transistors, light-emitting diodes, and photovoltaic cells, only a few examples of using conjugated polymers as photocatalysts to degrade toxic organic pollutants have been investigated.<sup>[16]</sup> The potential use of conjugated polymer photocatalysts in synthetic applications was illustrated by the visible-light-driven pinacol coupling of benzaldehyde by using PPP as a photoredox catalyst.<sup>[15]</sup> Additionally, PPP and visible light has been used to reduce water, carbon dioxide, ketones, keto esters, and electron-poor alkenes while promoting *cis-trans* isomerization.<sup>[15,17]</sup> The photofixation of CO<sub>2</sub> into benzophenone to yield benzylic acid was assisted by stronger reduction potentials of PPP.<sup>[17c]</sup> This has also spurred investigation into the photochemical reduction of CO<sub>2</sub> by PPP.<sup>[17k,17l]</sup> The change in the redox band potentials of conjugated polymers can have a profound influence on the reaction mechanism. For example, unlike TiO<sub>2</sub>, there was no evidence for the involvement of radical ions in the photoinduced *cis-trans* isomerization of alkenes promoted by PPP.<sup>[17a]</sup> Similarly, the reduction of maleate and fumarate to succinate was proposed to result from an initial one-electron reduction and subsequent disproportionation.<sup>[17m]</sup> In this work, a systematic investigation of the reaction mechanisms induced by PPP photocatalysis was undertaken. Using the photocatalysis of aryl aldehydes as a model system, the effect of varying the reaction conditions on the photocatalytic mechanisms were determined and ways to improve performance were identified.

## Results

The goal of this work was to examine how modifications to the photocatalytic conditions influenced reaction outcomes to gain insight into how to improve the system. In initial work by Yanagida and co-workers, benzaldehyde (**1**) exclusively underwent a pinacol coupling reaction to form hydrobenzoin (**2**) when PPP was irradiated with visible light in the presence of triethylamine (Et<sub>3</sub>N) as the sacrificial electron donor.<sup>[15]</sup> As shown in Scheme 2, a ketyl (**I<sub>k</sub>**) was proposed as the key intermediate in the mechanism. The hypothesis for this work was that putative **I<sub>k</sub>** could be diverted into a formal photoreduction to benzyl alcohol (**3**)

through the addition of a hydrogen atom donor, namely, a thiol. The effect of varying the initial concentrations of the starting reagents on the observed rates was investigated to elucidate the underlying mechanism and to identify where reaction optimization would have the greatest impact.



Scheme 2.

PPP was synthesized according to procedures described by Yamamoto and co-workers.<sup>[18]</sup> After preparation of the Grignard reagent of 1,4-dibromobenzene, the polymerization was catalyzed by nickel(II) dichloride bipyridine to afford a yellow slurry containing PPP. Soxhlet extraction with toluene yielded a yellow powder. Elemental analysis of several batches showed that the extracted PPP consisted of 74.5% carbon, 4.7% hydrogen, and 18.5% bromine on average. Using GPC analysis, the *M<sub>w</sub>* and *M<sub>n</sub>* was determined to be 500 Da and 363 Da, respectively, corresponding to a polydispersity of 1.38. If it is assumed that the polymerization was terminated by the reaction by a protic impurity, these values correspond with an average chain length of 5–6 benzene units with one end terminated by bromine (LMW-PPP). The insoluble material remaining after Soxhlet extraction consisted of higher molecular weight PPP (HMW-PPP), which was supported by elemental analysis. The insoluble PPP consisted, on average, of 84.5% carbon, 5.0% hydrogen, and 7.6% bromine, which would be consistent with a PPP chain of >7 phenylene units (HMW-PPP). Because the HMW-PPP material was completely insoluble, the molecular weight could not be determined by GPC. The UV spectrum of LMW-PPP dissolved in chloroform shows a single absorption band that extends past 400 nm with a maximum absorbance at 300 nm (Figure 1). In the previous reports, the  $\lambda_{\text{max}}$  for *p*-sexiphenyl as a solid was observed by reflectance spectrometry at 385 nm and when dissolved in THF at 317 nm.<sup>[19]</sup> Therefore, it was expected that as a solid the LMW-PPP would also absorb more of the visible spectrum.

Before examining the effect of a thiol hydrogen atom donor, the effect of different catalyst loadings and sacrificial electron donor (i.e., Et<sub>3</sub>N) concentrations on the pinacol coupling of benzaldehyde were investigated. In a typical experiment, the photolysis was carried out with eight fluorescent bulbs with an emission range of 400–440 nm. Disposable borosilicate glass test tubes (10 mL) were used as the reaction vessels, and oxygen was removed by argon sparging prior to irradiation. During photolysis, the reaction mixture was stirred constantly. The concentration of the starting aldehyde and the products was analyzed by using GC and GC–MS at 2 to 6 time points during irradiation. For these

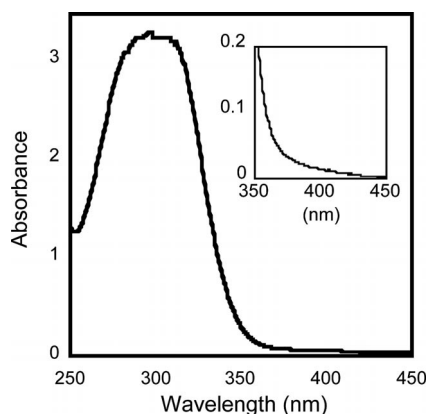


Figure 1. Absorption spectrum of low molecular weight PPP (LMW-PPP) dissolved in chloroform.

experiments, the initial concentration of **1** was held constant at ca. 5 mM, and the amounts of LMW-PPP and Et<sub>3</sub>N were varied. The only product identified was **2**, and a 75% mass balance was obtained. It also should be noted that a nearly equal amount of *meso* and *D/L* isomers of **2** was always obtained. A linear relationship between the rate of formation for **2** and the initial concentration of Et<sub>3</sub>N was found (Figure 2). As a practical matter, when less than 0.4 M of Et<sub>3</sub>N was used, the rate became too slow to measure accurately, and at very high concentrations, the quantity of Et<sub>3</sub>N complicated the chromatographic analysis. Thus, the remaining photocatalytic reactions were carried out at 1 M Et<sub>3</sub>N. As depicted in Figure 3, the rates of consumption of **1** and formation of **2** increased with the loading of LMW-PPP. For all experiments, a control under the same reaction conditions containing no PPP was irradiated for 24 h, upon which less than 5% conversion of **1** was always observed.

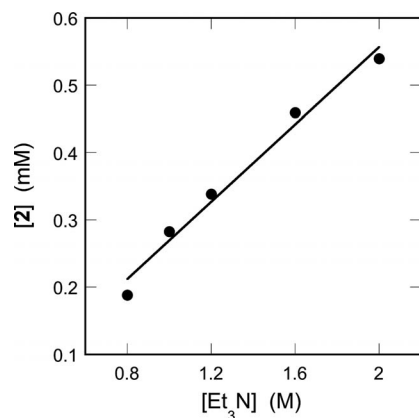


Figure 2. Concentration of hydrobenzoin (**2**) after 15 h of irradiation at 420 nm with varying concentrations of the Et<sub>3</sub>N, 5 mg of LMW-PPP, 5 mM **1** in acetonitrile.

The premise of this work was that modifications to the photocatalysis conditions would influence the observed products. Namely, the addition of hydrogen atom donors was expected to reduce the ketyl intermediate to the corresponding alcohol. Hydrogen abstraction from thiols by nucleophilic radicals is known to proceed rapidly.<sup>[20]</sup> Thus, the

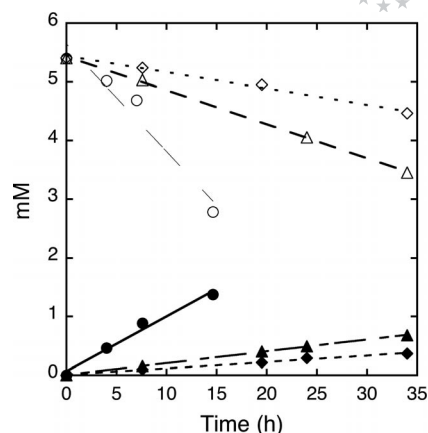


Figure 3. Concentration of benzaldehyde (**1**, open markers) and hydrobenzoin (**2**, solid markers) with 5 mg (diamond), 10 mg (triangle), and 10 mg washed and reused (circle) LMW-PPP upon irradiation at 420 nm with 1 M Et<sub>3</sub>N in acetonitrile.

products of the irradiation of **1** in the presence of 2-mercaptoethanol (BME), LMW-PPP, and Et<sub>3</sub>N were quantified. The photolysis products were analyzed by using GC and GC-MS. Products were identified as **2**, **3**, and the corresponding disulfide by comparison with authentic standards. The results of a typical photocatalytic reaction containing a thiol are depicted in Figure 4. The addition of BME increased the rate of consumption of **1**. The addition of other hydrogen atom donors (Brønsted acids) was also investigated to determine if the same results could be obtained. The substitution of acids for the thiol in the reaction resulted in the predominate formation of **2** rather than **3**. Subsequent study of the use of acid catalysis on this photoredox system was performed but is beyond the scope of this paper.

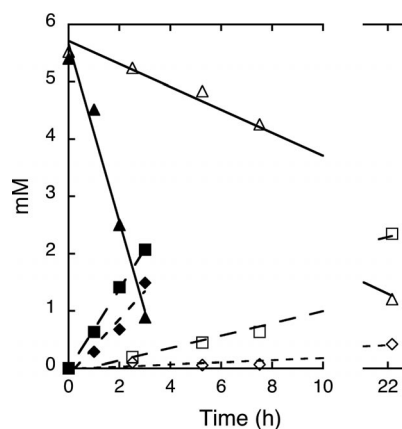


Figure 4. Concentration of **1** (triangle), **2** (diamond), and **3** (square) at different time points upon 420 nm irradiation of 10 mg of LMW-PPP, 500 mM 2-mercaptoethanol, and 1 M Et<sub>3</sub>N in acetonitrile. Open markers: first photolysis with unused LMW-PPP; closed markers: second run after LMW-PPP had been washed with acetonitrile and reused.

Unexpectedly, it was found that when LMW-PPP was reused, after sonicating and washing with acetonitrile, the photocatalytic activity increased. To investigate the cause of

## FULL PAPER

this observation, the solubility of the LMW-PPP photocatalyst was examined. When LMW-PPP was sonicated and left in acetonitrile overnight at 35 °C, 100% recovery of the mass of LMW-PPP was obtained after filtration and drying, and no solid residue was observed upon evaporation of the filtrate. This result indicated that LMW-PPP was insoluble in acetonitrile. To ensure the observed reactivity was not the result of some component of LMW-PPP being released into solution, LMW-PPP was removed by filtration from a typical photocatalytic reaction that had been allowed to proceed for 12 h to ca. 60% completion. After being degassed with argon, the filtrate was irradiated for another 8 h. Removal of the LMW-PPP resulted in the complete loss of photocatalytic activity. Complete loss of photocatalytic activity was also observed if LMW-PPP was removed by decantation after centrifugation immediately prior to irradiation. These control experiments indicated that the observed photocatalytic activity arose from catalysis on the surface of the LMW-PPP particles and was not the result of a molecular reductant or mediator.

To determine if the change in photocatalytic activity upon reuse was due to change in the LMW-PPP, the physical properties of LMW-PPP were examined before and after the photocatalytic reaction. The GPC data of PPP prior to and after photolysis were identical; however, elemental analysis showed a significant loss of bromine: 11.6% bromine prior to photolysis and 5.8% after photolysis. The drop in bromine content to 5.8% was similar to the bromine content typically found for the completely insoluble material (HMW-PPP) remaining after Soxhlet extraction. It should be noted that HMW-PPP could not be detected by GPC, as it is completely insoluble in all organic solvents. This led to the postulation that during photocatalysis the LMW-PPP was being transformed into a material similar to HMW-PPP. This hypothesis was examined by evaluating the photoreduction of **1** with LMW-PPP, the recycled material obtained by washing the used LMW-PPP (R-LMW-PPP), or HMW-PPP serving as the photoredox catalyst. As shown in Figure 5, the relative rates for the conversion of **1** increased roughly sixfold for HMW-PPP and R-LMW-PPP compared to unused LMW-PPP. Additionally, whereas **3** was the major product for LMW-PPP, **2** was the major product when HMW-PPP or R-LMW-PPP was used as the photocatalyst. Thus, the photocatalytic activity of the R-LMW-PPP was more similar to HMW-PPP than LMW-PPP.

The increase in rate observed for recycled LMW-PPP (R-LMW-PPP) suggested that an acceleration in the rate should occur during the course of the photolysis. However, no acceleration in the rate was detected for any single photocatalytic reaction performed during this study. One explanation for this observation was that the increase in photocatalytic activity was small over the course of a single photolysis to be observed. Thus, a series of 8-h photocatalytic reactions was performed by reusing the same LMW-PPP material (after being washed and dried) in each run (i.e., the R-LMW-PPP obtained from the initial LMW-PPP). In the absence of a thiol, a gradual increase in the rate of con-

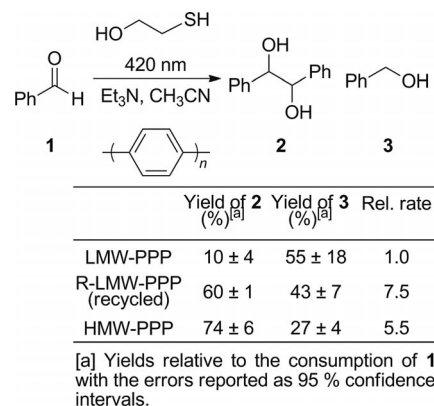


Figure 5. Irradiation of **1** (8 mM) at 420 nm in the presence of PPP (10 mg), 2-mercaptoethanol (500 mM), and Et<sub>3</sub>N (1 M) in acetonitrile.

sumption was observed from run to run. In the presence of 2-mercaptoethanol (500 mM), a very different result was obtained for a series of four 8-h irradiations reusing the same 10 mg of LMW-PPP throughout the series. Unlike in the absence of a thiol, the fourth run was only 1.5 times faster than the first, which was considerably slower than the 7.5-fold expected increase observed when LMW-PPP was reused from a photocatalytic reaction that proceeded to near completion (22 h). Elemental analysis of LMW-PPP after 8 h of (<33% conversion) revealed very little change (<2%) in the content of carbon and bromine. However, for a separate sample that was allowed to proceed for 21 h (90% conversion), a 10% increase in carbon content and concomitant loss of bromine was observed. Controls showed no change in elemental content upon washing with acetonitrile or if **1** was removed from the reaction mixture. Thus, the dramatic increase in the rate shown in Figures 4 and 5 was only observed when the initial photocatalysis was carried out to near complete conversion of starting material.

Because one of the objectives of this work was to divert aldehydes into undergoing photoreductions, the photocatalysis of **1** was carried out with 2-mercaptoethanol (BME), *tert*-butylthiol (*t*BuSH), 1-propanethiol (PrSH), benzyl mercaptan (BnSH), and ethyl 2-mercaptoacetate (EMA) by using virgin LMW-PPP. Additionally, it was observed that different batches of the PPP preparations had significant variability in their photocatalytic activity (±30%), as measured by the consumption rate of **1**. Thus, unless stated otherwise, comparisons were only made with LMW-PPP from the same preparation, which was not reused, to reduce the variance of the observed reaction rates. The relative rates and the product yields of **2** and **3** relative to the consumption of **1** in the presence of BME, PrSH, *t*BuSH, BnSH, or EMA are reported in Table 1. The average combined product yield of **2** and **3** was near 70%, and every thiol was capable of inducing the photoreduction of **1** to **3**. The best yields of **3** were obtained with EMA; however, compared to the absence of the additive thiol, BME, EMA, and BnSH accelerated the reaction, whereas PrSH and



*t*BuSH had little effect or decreased the rate of reaction. Photolysis with *t*BuSH added afforded a 1:3 alcohol to pinacol ratio. A Brønsted plot of the consumption rate of **1** and the  $pK_a$  values of the thiols (Figure 6) was used to determine if there was any relationship with the acidity of the thiols examined. Decent correlation between the reaction rates and the  $pK_a$  values of the thiols was evident.

Table 1. Benzaldehyde (**1**) PPP photocatalysis with various thiols.<sup>[a]</sup>

Entry	Thiol <sup>[a]</sup>	$pK_a$	Rel. rate <sup>[b]</sup>	Conv. (%) of <b>1</b> in 15 h	Yield (%) <b>2</b> <sup>[c]</sup>	Yield (%) <b>3</b> <sup>[d]</sup>
1	None	—	1.0	21.2	83 ± 14 <sup>[e]</sup>	none
2	EMA	8.0 <sup>[f]</sup>	4.5	95.2	none	85 ± 5
3	BnSH	9.4 <sup>[f]</sup>	1.9	40.2	10 ± 3	48 ± 7
4	BME	9.6 <sup>[f]</sup>	2.2	46.5	24 ± 7	50 ± 5
5	PrSH	10.5 <sup>[f]</sup>	1.0	21.2	23 ± 11	50 ± 12
6	<i>t</i> BuSH	11.4 <sup>[f]</sup>	0.8	16.9	42 ± 11	21 ± 7

[a] 500 mM thiol concentration, 420 nm irradiation of 10 mg of LMW-PPP, 5 mM of **1**, and 1 M Et<sub>3</sub>N in acetonitrile. [b] Averaged relative rates for the conversion of **1** by using LMW-PPP from same preparation. [c] Yield of **2** relative to the consumption of **1**. [d] Yield of **3** relative to the consumption of **1**. [e] 95% confidence interval. [f] Ref.<sup>[21]</sup>

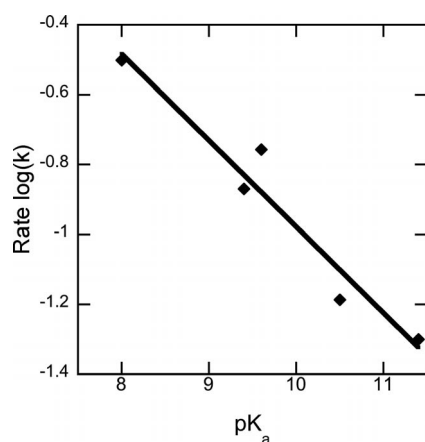


Figure 6. Rate of consumption of **1** (log) vs.  $pK_a$  of thiols used. Photolysis carried out by using 420 nm irradiation of 10 mg of LMW-PPP, ≈5 mM benzaldehyde, 500 mM thiol, and 1 M Et<sub>3</sub>N in acetonitrile.

The effect of thiol concentration on photolysis on the reaction was also examined. Identical solutions were prepared except the starting concentration of the thiol was varied from 20 to 500 mM. The samples were allowed to react for 19 h followed by analysis of the products. As depicted in Figure 7, no definitive trend was observed for **2**. However, there was a linear correlation between the thiol concentration and the amount of **3** formed after 19 h of photolysis. Because there was a linear relationship with respect to thiol concentration, the change in the concentration of **3** can be directly correlated to the rate of formation. Consistent with the data in Table 1, the magnitude of the slope for BME was greater than the slope for *t*BuSH.

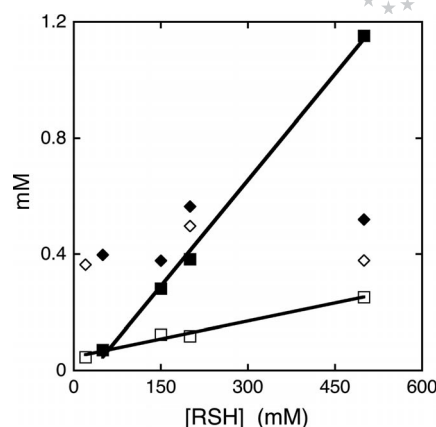


Figure 7. Concentration of products **2** (diamonds) and **3** (squares) vs. the starting concentration of 2-mercaptoethanol (closed markers) or *tert*-butylthiol (open markers) after 19 h of 420 nm irradiation with 10 mg of LMW-PPP, 5 mM of **1**, and 1 M Et<sub>3</sub>N in acetonitrile.

In a control experiment, it was unexpectedly observed that photoreduction of **1** occurred in the absence of the Et<sub>3</sub>N sacrificial donor, albeit at a much slower rate. To examine if the thiols could serve as the sacrificial electron donor, the photolysis was carried out at different concentrations of BME without any Et<sub>3</sub>N. Indeed, as shown in Table 2, an increase in the relative rates of the formation of **3** was observed as the concentration of BME increased. A similar trend was observed for **2**; however, at very high concentrations of the thiol, **2** could not be detected. The addition of Et<sub>3</sub>N (1 M) resulted in an eightfold increase in the overall rate. These results indicated that BME acted as a sacrificial electron donor.

Table 2. Comparison of rates with and without Et<sub>3</sub>N.

Entry	Thiol (mM) <sup>[a]</sup>	Rel. rate <b>2</b> <sup>[b]</sup>	Rel. rate <b>3</b> <sup>[b]</sup>
1	0	n.d. <sup>[c]</sup>	n.d. <sup>[c]</sup>
2	20	1.0	2.2
3	50	0.6	3.7
4	150	1.2	4.3
5	200	3.1	5.5
6	500	n.d. <sup>[c]</sup>	10.1
7	0 <sup>[d]</sup>	22.1	n.d. <sup>[c]</sup>
8	500 <sup>[d]</sup>	31.1	35.0

[a] 2-Mercaptoethanol concentration. [b] Relative rates for the formation of the products irradiated with 420 nm light, 10 mg of LMW-PPP in acetonitrile. [c] Not detected. [d] 1 M Et<sub>3</sub>N.

For interfacial charge transfer to compete with facile charge carrier recombination, pre-adsorption of the substrate to the surface was assumed necessary. To examine the effect of adsorption of **1** to LMW-PPP, a set of photocatalytic reactions with increasing starting concentrations of **1** and constant BME (250 mM) were performed. Unlike when the concentration of Et<sub>3</sub>N, PPP, or thiol was varied, a relatively large variance in the rates was observed when the concentration of **1** was varied, even within the same LMW-PPP preparation. In Figure 8, each data point represents the average of a minimum of four runs at equal starting concentrations of **1**. The rate data was collected from three dif-

## FULL PAPER

ferent PPP preparations, which likely accounts for some of the error. Additionally, at high concentrations of **1**, the change in concentration was small relative to the starting concentration, which also increased the observed error. As shown in Figure 8, varying the concentration of **1** resulted in saturation kinetics. Namely, the reactions exhibited a change from pseudo-first-order at low substrate concentration to near zero-order at high concentration. This is typical for heterogeneous photocatalytic reactions and does not necessitate a change in mechanism.<sup>[18]</sup> Langmuir–Hinshelwood kinetics are commonly used to describe these photocatalytic systems, which assumes that the substrate partitioning between the surface and solution are at equilibrium. Thus, the rate is dependent upon the extent of surface coverage,  $\theta$ , as defined in Equation (1), where  $K_c$  is the adsorption coefficient. The observed rate is then proportional to the extent of surface coverage as defined by Equation (2), where  $k_{LH}$  is the concentration-independent photocatalytic rate constant and  $[1]_0$  is the initial concentration of **1**.<sup>[22]</sup> A least-squares curve fit was used to determine  $K_c$  ( $8.8 \times 10^{-5} \text{ M}^{-1}$ ) and  $k_{LH}$  [ $k_{LH}$  (benzaldehyde) =  $1.2 \times 10^6 \text{ s}^{-1}$ ;  $k_{LH}$  (hydrobenzoin) =  $1.5 \times 10^5 \text{ s}^{-1}$ ;  $k_{LH}$  (benzyl alcohol) =  $4.1 \times 10^5 \text{ s}^{-1}$ ] for the substrates and products.

$$\theta = K_c [1]_0 / (1 + K_c [1]_0) \quad (1)$$

$$\text{rate} = k_{LH} \theta = k_{LH} K_c [1]_0 / (1 + K_c [1]_0) \quad (2)$$

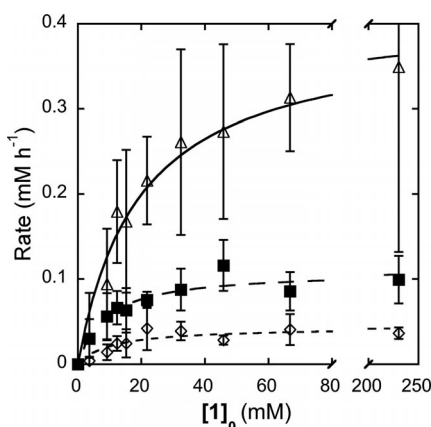


Figure 8. Rates for the loss of **1** (triangles) and the formation of **2** (diamonds) and **3** (squares) at different starting concentrations of **1**. Photocatalysis carried out with 420 nm irradiation, 10 mg of PPP, 250 mM of 2-mercaptoethanol (BME), and 1 M Et<sub>3</sub>N. Error bars represent 95% confidence interval for **2** and **3** and 80% for **1**. Curves were obtained by a least square fit of Equation 2.

To study electronic effects on the photocatalytic redox system, a series of 4-substituted benzaldehydes were photolyzed with and without BME (500 mM). Except for 4-acetylbenzaldehyde, the products of the reaction were identified as the corresponding pinacols and benzyl alcohols by comparison to authentic standards. As seen in Table 3, electron-donating substituents decrease the yield and rate of pinacol formation in the absence of the thiol, and no alcohol was observed. Conversely, electron-withdrawing substituents in-

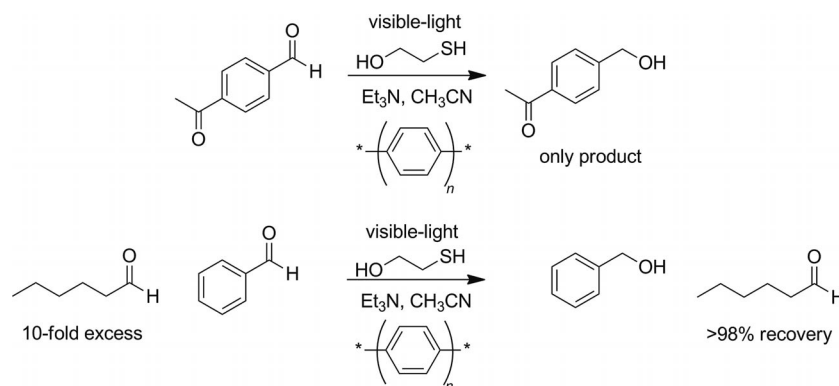
creased the overall rate of reaction compared to benzaldehyde, and in the case of moderately deactivating 4-acetylbenzaldehyde, the corresponding alcohol was detected as a minor product. In all cases, the addition of a thiol increased the rate of consumption of the aryl aldehyde.

Table 3. PPP photocatalysis of 4-substituted benzaldehydes in the presence and absence of 2-mercaptoethanol (BME).<sup>[a]</sup>

Entry	R	BME (mM) <sup>[b]</sup>	Rel. rate <sup>[c]</sup>	Conv. (%) of SM in 23 h	Yield (%) pinacol <sup>[d]</sup> alcohol <sup>[e]</sup>
1 <sup>[f]</sup>	H	0	1.0	43.2	76 ± 7 <sup>[g]</sup> n.d. <sup>[h]</sup>
2 <sup>[f]</sup>	H	500	1.6	69.2	19 ± 1 51 ± 10
3	Me	0	0.6	25.9	67 ± 10 n.d. <sup>[h]</sup>
4	Me	500	1.1	47.6	11 ± 2 83 ± 6
5	MeO	0	0.4	17.3	44 ± 3 n.d.
6	MeO	500	0.9	38.9	n.d. <sup>[h]</sup> 98 ± 2
7	F	0	1.7	73.5	89 ± 12 n.d. <sup>[h]</sup>
8	F	500	2.2	95.1	18 ± 5 70 ± 15
9	COMe	0	2.0	86.5	52 ± 28 <sup>[i]</sup> 18 ± 7
10	COMe	500	2.2	95.1	n.d. <sup>[h]</sup> 84 ± 1
11	OH	0	—	—	n.d. <sup>[h]</sup> n.d. <sup>[h]</sup>
12	OH	500	1.9	82.2	n.d. <sup>[h]</sup> 100 ± 1

[a] Photocatalysis carried out with 420 nm, 10 mg of LMW-PPP, and 1 M Et<sub>3</sub>N. The LMW-PPP was all from the same preparation for all runs. [b] 2-Mercaptoethanol concentration. [c] Relative rates for the consumption of **1**. [d] Yield of the corresponding pinacol coupling product relative to the conversion of aldehyde. [e] Yield of the corresponding benzyl alcohol relative to the conversion of aldehyde. [f] Discrepancy in rates from Table 1 a result of using different PPP from different preparations. [g] 95% confidence interval. [h] Not detected. [i] Calibration curve sensitivity was estimated as the average value of the other pinacol products.

In the photocatalysis of 4-acetylbenzaldehyde with thiols, only 4-acetylbenzyl alcohol was detected, which was verified by comparison to an authentic standard. Because 4-(1-hydroxyethyl)benzaldehyde was not detected, the LMW-PPP photocatalytic system was used to achieve the chemoselective reduction of an aryl aldehyde in the presence of an aryl ketone. In the absence of a thiol, GC–MS analysis revealed four different peaks with a  $m/z$  consistent with the pinacol coupling of 4-acetylbenzaldehyde. This was taken as an indication that the *meso* and *D/L* isomers of two out of the three possible pinacol couplings (aldehyde/aldehyde, aldehyde/ketone, ketone/ketone) were formed. Attempts to isolate these products were thwarted by instability of these products towards column chromatography. The instability of these products also contributed to the larger variation reported in entry 9 of Table 3. The calibration curve sensitivity of our GC analysis for the various pinacol coupling products was fairly consistent, and thus, the concentration of these products was estimated by averaging the calibration curves of the other pinacols. Additionally, it was examined if benzaldehyde could be reduced in the presence of an aldehyde with a higher reduction potential, hexanal, to see if selectivity could be achieved. A series of mixed aldehyde



Scheme 3.

experiments with benzaldehyde and hexanal, where the amount of hexanal was varied from equimolar to 10-fold excess, were performed. As shown in Scheme 3, the only products obtained from these experiments were **2** and **3**, and no hexanol or pinacol coupling products involving hexanal were observed. For both cases shown in Scheme 3, the aryl aldehyde was selectively reduced consistent with its less negative reduction potential. This indicates that other chemoselective reductions could be achieved by tailoring the redox potential of PPP or other conjugated polymer photoredox catalysts.

## Discussion

The structural variety, distinctive redox potentials, and the absorption of visible light make conjugated polymers attractive photoredox catalysts. Given the previously reported pinacol coupling of **1** by PPP photocatalysis and visible light, aryl aldehydes were a reasonable model system to begin the investigation of conjugated polymers as photoredox catalysts.<sup>[15]</sup> The proceeding results support the working hypothesis that the addition of a hydrogen donor was able to trap putative ketyl **I<sub>k</sub>** leading to a formal photoreduction of **1** (Scheme 2). Because electron-hole annihilation is energetically favorable, pre-adsorption of **1** to the surface of PPP was an expected necessity for efficient interfacial electron transfer. The observed saturation kinetics with respect to **1** shown in Figure 8 was consistent with the expectation of heterogeneous catalysis.<sup>[23]</sup> Additionally, the loss of any photocatalytic activity upon the removal of PPP supports the postulation that the reduction of **1** occurs by interfacial electron transfer at the surface and not due to a mediator or some miniscule amount of dissolved LMW-PPP. Analysis of the Langmuir–Hinshelwood kinetics found a very low value for  $K_c$  ( $10^{-5} \text{ M}^{-1}$ ). This low  $K_c$  suggested that binding of **1** to the catalytic surface was weak, and thus, poor adsorption of **1** to the PPP surface was likely a significant factor limiting the rate of photocatalysis.

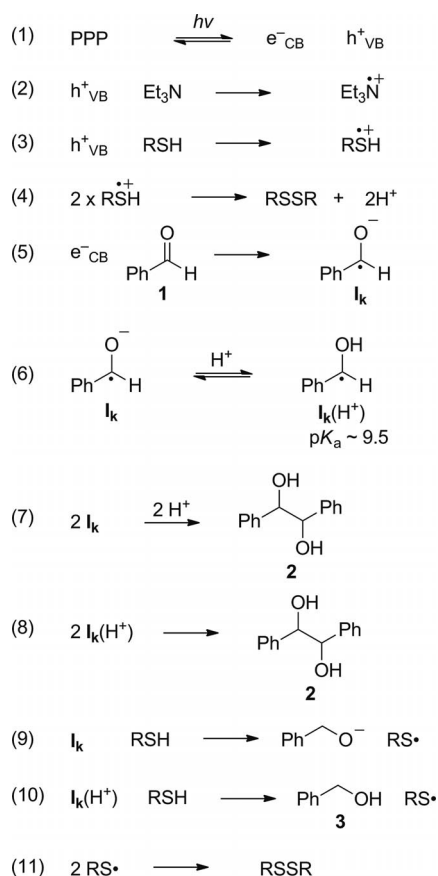
In the absence of a thiol, the consumption of **1** was fairly inefficient, and thus, improvement of the photocatalytic properties of PPP is desirable. The conduction band potential of PPP prepared in the same fashion was reported as  $-2.0 \text{ V}$  vs. NHE, and thus, electrons in the conduction band

were expected to reduce benzaldehyde ( $-1.69$  vs. NHE).<sup>[24]</sup> As with any photochemical reaction, the rate of photoredox catalysis increases with greater photon flux, and therefore, greater absorption efficiency would also be expected to increase rates. Spectral characterization (UV/Vis) of dissolved LMW-PPP in chloroform shown in Figure 1 revealed only minimal absorption in the visible region. The low absorbance in the visible ranges indicated PPP photocatalysts would benefit by increasing the efficiency of absorption in this region. For most semiconductor photocatalysts, energy wasting electron-hole annihilation is the dominant non-productive processes competing with productive interfacial charge transfer.<sup>[25]</sup> Therefore, efficient trapping of charge carriers is essential to photocatalysis. The first-order dependence of the rate of formation of **2** in respect to  $\text{Et}_3\text{N}$  up to  $2 \text{ M}$  suggested that non-productive processes involving  $\text{h}^+_{\text{VB}}$  were occurring. Because pre-adsorption was an expected requirement to compete with electron-hole annihilation, the high concentrations of  $\text{Et}_3\text{N}$  required for catalytic activity suggested that association of the amine with the catalytic surface was weak. A sacrificial electron donor with stronger binding would be expected to more efficiently trap  $\text{h}^+_{\text{VB}}$ .

The addition of thiols to the photolysis mixture diverted aryl aldehydes into undergoing a formal photoreduction rather than the pinacol coupling reaction observed in the absence of thiols. As shown for the proposed mechanism in Scheme 4, reduction of the aldehyde by a light-promoted conduction band electron was expected to generate putative ketyl intermediate **I<sub>k</sub>** (Scheme 4, line 5). The self-coupling and protonation of **I<sub>k</sub>** would yield **2** (Scheme 4, line 7). An argument against **I<sub>k</sub>** reacting with **1** from the bulk solution leading to **2** is the independence of the product ratio with respect to the starting concentration of **1**. When the thiol concentrations are held constant, the ratio of **2** to **3** should increase proportionally with the initial concentration of **1** if pinacol coupling arose from a reaction of **I<sub>k</sub>** with bulk **1**. However, the ratio of **2** to **3** did not change once surface saturation was reached in Figure 8 where the rate for the formation of **I<sub>k</sub>** would be constant. The addition of a thiol was expected to provide a competing pathway to self-coupling, as hydrogen abstraction from thiols by carbon-centered radicals is diffusion controlled.<sup>[20]</sup> The formation of **3** was consistent with **I<sub>k</sub>** abstracting a hydrogen atom from

## FULL PAPER

the added thiol (Scheme 4, line 9). As shown in line 11 (Scheme 4), the resulting sulfonyl radicals form disulfides at diffusion controlled rates.<sup>[26]</sup> The rate-limiting step was expected to be interfacial electron transfer, and thus, an unanticipated result was the increase in the overall rate of the reaction for some of the examined thiols (Table 1, entries 2–4). A potential explanation was that these thiols prevented charge carrier recombination, which was possible because 2-mercaptoethanol (BME) acted as the sacrificial electron donor in the absence of Et<sub>3</sub>N. However, this explanation was deemed unlikely because the conversion of **1** in the absence of Et<sub>3</sub>N occurred at only 10% of the rate observed under our standard conditions (Table 2 entries 6 & 8), whereas the rate doubled when BME was added (Table 2, entries 7 & 8). If the addition of thiols only prevented e<sup>−</sup><sub>CB</sub>/h<sup>+</sup><sub>VB</sub> recombination, a much smaller increase in the rate of consumption of **1** would have been anticipated.



Scheme 4. Proposed mechanism.

As shown in Figure 6, a Brønsted plot demonstrated a linear relationship between the overall rates and the pK<sub>a</sub> values of the examined thiols. The pK<sub>a</sub> value of the protonated ketyl radical [**I<sub>k</sub>(H<sup>+</sup>)**] has been estimated to lie between 8.4 and 10.5, and thus, protonation of **I<sub>k</sub>** by the examined thiols was possible.<sup>[27]</sup> Given the redox potentials of **I<sub>k</sub>**, h<sup>+</sup><sub>VB</sub>, and Et<sub>3</sub>N<sup>•+</sup>, back electron transfer from **I<sub>k</sub>** to PPP (h<sup>+</sup><sub>VB</sub>) or Et<sub>3</sub>N<sup>•+</sup> would not be surprising. Protonation of **I<sub>k</sub>** decreases the oxidation potential of the ketyl and concomitantly increases the lifetime of **I<sub>k</sub>(H<sup>+</sup>)**, which would fa-

cilitate the reductive couplings reactions in lines 8 and 10 (Scheme 4). These results indicate that the observed acceleration in the overall rate upon the addition of acidic thiols was largely due to their ability to protonate **I<sub>k</sub>** and only partially by acting as sacrificial electron donor (Scheme 4, line 3). As expected based on their pK<sub>a</sub> values, the overall rate was largely unaffected by the addition of *t*BuSH and PrSH, which was consistent with the assumption that they do not substantially protonate **I<sub>k</sub>**.

As expected, an increase in the concentration of a thiol led to an increase in the rate of formation of **3** as shown in Figure 7. Because the bond strength of the S–H bond was expected to correlate with the pK<sub>a</sub>, it was expected that thiols with lower pK<sub>a</sub> values would be better hydrogen atom donors and yield greater ratios of **3** to **2**.<sup>[28]</sup> This trend was observed for BME, BnSH, and EMA and also can be used to explain PrSH vs. *t*BuSH. However, PrSH and BME yielded a similar ratio of **3** relative to **2**, which was reflective of their different mechanisms. For the more acidic thiols (BME, BnSH, EMA), their ability to protonate **I<sub>k</sub>** accelerates the overall reaction with a concomitant increase in the amount of **I<sub>k</sub>(H<sup>+</sup>)**. Because pinacol coupling (Scheme 4, line 8) increases to the second power of the concentration **I<sub>k</sub>(H<sup>+</sup>)** and hydrogen abstraction from the thiol increases linearly (Scheme 4, line 10), an increase in the rate of **I<sub>k</sub>(H<sup>+</sup>)** generation favors the formation of **2**. Likewise, the same explanation of increased **I<sub>k</sub>(H<sup>+</sup>)** formation can be applied to explain the increased amount of **2** compared to **3** for HMW-PPP in the presence of BME, as HMW-PPP is more active (Figure 5). Propanethiol and *tert*-butylthiol were not expected to protonate **I<sub>k</sub>**, and thus, they have little or a negative effect on the amount of **I<sub>k</sub>** being created. Thus, the addition of PrSH or *t*BuSH simply provides a hydrogen atom abstraction pathway that competes with pinacol coupling of **I<sub>k</sub>**. The increased sterics and increased S–H bond dissociation for *t*BuSH most likely hinders the hydrogen abstraction pathway leading to **3**, which accounts for **2** being the major product.

In the absence of thiols, electron-donating groups slow the rate of aldehyde consumption and the formation of the corresponding hydrobenzoin. This was consistent with the interfacial charge transfer becoming less energetically favorable. Group 16 hydrogen atom donors react faster with nucleophilic radicals, and thus, electron-rich ketyl intermediates were expected to react faster with thiols, which hinders pinacol coupling and back electron transfer.<sup>[20a]</sup> Conversely, thiols were not able to completely prevent pinacol coupling of benzaldehyde and 4-fluorobenzaldehyde. A plausible explanation is that electron-withdrawing substituents ease the initial reduction leading to **I<sub>k</sub>**, which again increases the effective concentration of **I<sub>k</sub>**.

Another interesting result was the improved photocatalytic activity observed for the reused LMW-PPP (R-LMW-PPP), which correlated with a significant decrease in the bromine content of the material. This indicated that the LMW-PPP was being modified at the molecular level. Comparison of photocatalytic and physical properties revealed that R-LMW-PPP was more similar to the HMW-PPP ma-



terial than starting unused LMW-PPP from which it was obtained. Therefore, a reasonable explanation for the increased rate of photocatalysis was the transformation of LMW-PPP into a material similar to HMW-PPP by the formation of C–C bonds between the PPP units during the course of the reaction. In the presence of a thiol, the transformation of LMW-PPP into a material similar to HMW-PPP accelerated after near complete conversion of the starting material, and thus, much of the transformation of PPP occurred after the reaction was complete. An increasing rate of PPP transformation at high conversion of **1** was consistent with the observation that no increase in the rate of photocatalysis was observed over the course of a single reaction during this study. Because the relative rates were determined for reactions proceeding to less than 40% conversion with unused LMW-PPP from the same preparation, the relative rates provided a valid method of evaluating the effects of modifications to the reaction conditions on photocatalysis.

## Conclusions

Irradiation of PPP with visible light in the presence of a sacrificial electron donor was able to catalyze the one-electron reduction of aryl aldehydes to generate a ketyl intermediate. The ketyl intermediate undergoes a pinacol coupling reaction on the surface of the photocatalyst competitively with non-productive back electron transfer. In the presence of thiol hydrogen atom donors, the ketyl intermediate can be diverted into a formal photoreduction by abstracting a hydrogen atom from the thiol to form an alcohol. The chemoselective reduction of aryl aldehydes over alkyl aldehydes and aryl ketones was also achieved. As expected, aryl aldehydes with lower reduction potentials were more reactive towards photocatalysis. The conjugated polymer photocatalysts could be reused by sonicating and rinsing with acetonitrile, which resulted in an increase in photocatalytic activity. The rate of photocatalysis was hindered by inefficient absorbance, poor binding to surface by the substrate, and an unoptimized sacrificial electron donor.

## Experimental Section

**Materials:** 1,4-Dibromobenzene, benzaldehyde, 4-methylbenzaldehyde, 4-methoxybenzaldehyde, 4-hydroxybenzaldehyde, 4-fluorobenzaldehyde, benzyl alcohol, 4-methylbenzyl alcohol, 4-methoxybenzyl alcohol, 4-fluorobenzyl alcohol, 4-hydroxybenzyl alcohol, hydrobenzoin, NiCl<sub>2</sub>, 2,2'-bipyridine, 2-octanol, and triethylamine were purchased from Sigma–Aldrich or Fisher Scientific and used as received without further purification. NiCl<sub>2</sub>(bpy) was prepared from NiCl<sub>2</sub> and 2,2'-bipyridine according to the reported procedure.<sup>[29]</sup> Poly(*p*-phenylene) was synthesized by Yamamoto's method.<sup>[31]</sup> A slightly modified literature procedure was used to prepare 1,2-bis(4-methylphenyl)-1,2-ethanediol, 1,2-bis(4-methoxyphenyl)-1,2-ethanediol, and 1,2-bis(4-fluorophenyl)-1,2-ethanediol.<sup>[30]</sup>

**Irradiations:** The photolysis reactions were carried out in HPLC-grade acetonitrile, which was used without further purification.

Photocatalytic reactions were carried out by using a LZ4-X Luzchem Photoreactor with eight fluorescent bulbs generating approximately 70 W m<sup>−2</sup> from 400–440 nm. As noted in the text, starting concentrations of the aryl aldehydes were varied from 1 to 250 mM; however, typical experiments were run at 5 mM. Solutions of the starting aryl aldehyde, triethylamine (1 M), thiol (0–500 mM), and PPP (10 mg) were placed into a borosilicate test tube for photolysis. Prior to photolysis, all of the samples were sparged with argon for at least 30 min and sonicated to break up the heterogeneous PPP powder. During the photoreaction, the samples were stirred and the temperature was held constant at 25–30 °C. The products analysis was performed by periodic GC analysis by using a Hewlett–Packard 5890 Series II GC fitted with a flame ionization detector and DB-5 column. The internal standards used for GC quantifying the aryl aldehydes and products were 2-octanol and dodecane. For products not amenable to GC analysis, an Agilent 1100 Series HPLC fitted with a UV/Vis diode array detector and Eclipse XDB-C18 column was used. Control reactions were performed where one variable (light, PPP, or Et<sub>3</sub>N) was removed. Less than 5% loss of the starting material was observed for all of these controls.

**General Methods:** Ultraviolet absorbance spectra were collected with a Shimadzu PharmaSpec UV-1700. GPC analysis was performed by using Agilent 1100 Series HPLC fitted with a UV/Vis diode array detector and Shodex LF-404 temperature-controlled column by using chloroform. A Bruker 400 MHz Broadband NMR spectrometer with a direct probe was used to collect proton signal for all of the prepared compounds. A Shimadzu GC–MS QP2010S was used to collect molecular fragmentation information for initial identification of possible photoproducts. For elemental analysis, compounds were sent to Atlantic Microlabs (Norcross, GA, USA) for C, H, and Br content.

**Supporting Information** (see footnote on the first page of this article): Copies of the <sup>1</sup>H NMR, <sup>13</sup>C NMR, and mass spectra of compounds 1,2-bis(4-fluorophenyl)-1,2-ethanediol, 1,2-bis(4-methoxyphenyl)-1,2-ethanediol, and 1,2-bis(4-methylphenyl)-1,2-ethanediol.

## Acknowledgments

The authors thank the donors of the Beaumont Faculty Development Fund for support of this work.

- [1] a) N. Hoffmann, *Chem. Rev.* **2008**, *108*, 1052; b) J. M. R. Narayanam, C. R. Stephenson, *J. Chem. Soc. Rev.* **2011**, *40*, 102.
- [2] a) P. V. Pham, D. A. Nagib, D. W. C. MacMillan, *Angew. Chem. Int. Ed.* **2011**, *50*, 6119; b) Z. Lu, M. Shen, T. P. Yoon, *J. Am. Chem. Soc.* **2011**, *133*, 1162; c) J. W. Tucker, C. R. Stephenson, *Org. Lett.* **2011**, *13*, 5468; d) J. W. Tucker, J. M. R. Narayanam, S. W. Krabbe, C. R. Stephenson, *Org. Lett.* **2010**, *12*, 368; e) A. G. Condie, J. C. González-Gómez, C. R. Stephenson, *J. Am. Chem. Soc.* **2010**, *132*, 1464; f) J. M. R. Narayanam, J. W. Tucker, C. R. J. Stephenson, *J. Am. Chem. Soc.* **2009**, *131*, 8756; g) J. Du, T. P. Yoon, *J. Am. Chem. Soc.* **2009**, *131*, 14604; h) D. A. Nicewicz, D. W. C. MacMillan, *Science* **2008**, *322*, 77; i) M. A. Ischay, M. E. Anzovino, J. Du, T. P. Yoon, *J. Am. Chem. Soc.* **2008**, *130*, 12886; j) D. Nagib, M. Scott, D. MacMillan, *J. Am. Chem. Soc.* **2009**, *131*, 10875; k) T. Maji, A. Karmakar, O. Reiser, *J. Org. Chem.* **2011**, *76*, 736.
- [3] a) N. J. Hoffmann, *Photochem. Photobiol. C* **2008**, *9*, 43; b) D. P. Hari, B. König, *Org. Lett.* **2011**, *13*, 3852.
- [4] a) G. Palmisano, E. Garcia-Lopez, G. Marci, V. Loddo, S. Yurdakal, V. Augugliaro, L. Palmisano, *Chem. Commun.* **2010**, *46*, 7074; b) M. A. Fox, M. T. Dulay, *Chem. Rev.* **1993**, *93*, 341; c)

## FULL PAPER

M. Zhang, W. D. Rouch, R. D. McCulla

- T. Tachikawa, M. Fujitsuka, T. Majima, *J. Phys. Chem. C* **2007**, *111*, 5259; d) M. Cherevatskaya, M. Neuman, S. Földner, C. Harlander, S. Kümmel, S. Dankesreiter, A. Pfützner, K. Zeitler, B. König, *Angew. Chem.* **2012**, *124*, 4138; *Angew. Chem. Int. Ed.* **2012**, *51*, 4062.
- [5] a) N. M. Ghazzal, N. Chaoui, E. Aubry, A. Koch, D. Robert, *J. Photochem. Photobiol. A: Chem.* **2010**, *215*, 11; b) W. S. Jenks in *Environmental Catalysis* (Ed.: V. H. Grassian), CRC Press, Boca Raton, FL, **2005**, vol. 1, p. 307.
- [6] R. Jahjah, A. Gassama, F. Dumur, S. Marinkovic, S. Richert, S. Landgraf, A. Lebrun, C. Cadiou, P. Selles, N. Hoffmann, *J. Org. Chem.* **2011**, *76*, 7104.
- [7] a) H. Kominami, H. Sugahara, H. Hashimoto, *Catal. Commun.* **2010**, *11*, 426; b) M. Zhang, Q. Wang, C. Chen, L. Zhang, W. Ma, J. Zhao, *Angew. Chem.* **2009**, *121*, 6197; *Angew. Chem. Int. Ed.* **2009**, *48*, 6081; c) A. Molinari, M. Bruni, A. Maldotti, *J. Adv. Oxid. Technol.* **2008**, *11*, 143; d) A. Molinari, M. Montoncello, H. Rezala, A. Maldotti, *Photochem. Photobiol. Sci.* **2009**, *8*, 613; e) S. Higashimoto, N. Kitao, N. Yohida, Y. Sakura, M. Azuma, H. Ohue, Y. Sakata, *J. Catal.* **2009**, *266*, 279; f) C. Minero, G. Mariella, V. Maurino, E. Pelizzetti, *Langmuir* **2000**, *16*, 2632.
- [8] a) G. Palmisano, S. Yurdakal, V. Augugliaro, V. Loddo, L. Palmisano, *Adv. Synth. Catal.* **2007**, *349*, 964; b) V. Loddo, S. Yurdakal, G. Palmisano, G. E. Imoberdorf, H. A. Irazoqui, O. M. Alfano, V. Augugliaro, H. Berber, L. Palmisano, *Int. J. Chem. React. Eng.* **2007**, *5*, A57; c) S. Yurdakal, G. Palmisano, V. Loddo, V. Augugliaro, L. Palmisano, *J. Am. Chem. Soc.* **2008**, *130*, 1568; d) M. Addamo, V. Augugliaro, M. Bellardita, A. Di Paola, L. Loddo, G. Palmisano, L. Palmisano, S. Yurdakal, *Catal. Lett.* **2008**, *126*, 58; e) V. Augugliaro, T. Caronna, V. Loddo, G. Marci, G. Palmisano, L. Palmisano, S. Yurdakal, *Chem. Eur. J.* **2008**, *14*, 4640; f) S. Yurdakal, V. Loddo, G. Palmisano, V. Augugliaro, H. Berber, L. Palmisano, *Ind. Eng. Chem. Res.* **2010**, *49*, 6699.
- [9] a) P. Kluson, H. Luskova, L. Cerveny, J. Klisakova, T. Cajtham, *J. Mol. Catal. A* **2005**, *242*, 62; b) T. Klisakova, P. Kluson, L. Cerveny, *Collect. Czech. Chem. Commun.* **2003**, *68*, 1985; c) C. Murata, H. Yoshida, J. Kumagai, T. Hattori, *J. Phys. Chem. B* **2003**, *107*, 4364.
- [10] a) P. Du, J. A. Moulijn, G. Mul, *J. Catal.* **2006**, *238*, 342; b) A. Maldotti, A. Molinari, R. Amadelli, E. Carbonell, H. Garcia, *Photochem. Photobiol. Sci.* **2008**, *7*, 819; c) M. Alvaro, C. Aprile, E. Benitez, E. Carbonell, H. Garcia, *J. Phys. Chem. B* **2006**, *110*, 6661.
- [11] M. A. Fox, B. Lindig, C. C. Chen, *J. Am. Chem. Soc.* **1982**, *104*, 5828.
- [12] M. A. Fox, B. Lindig, C. C. Chen, *J. Am. Chem. Soc.* **1981**, *103*, 6757.
- [13] M. A. Fox, M. J. Chen, *J. Am. Chem. Soc.* **1983**, *105*, 4491.
- [14] W. Dunn, Y. Aikawa, A. Bard, *J. Am. Chem. Soc.* **1981**, *103*, 3456.
- [15] a) T. Shiragami, A. Kabumoto, O. Ishitani, C. Pac, S. Yanagida, *J. Phys. Chem.* **1990**, *94*, 2068.
- [16] a) C. Wen, K. Hasegawa, T. Kanbara, S. Kagaya, T. Yamamoto, *J. Photochem. Photobiol. A: Chem.* **2000**, *137*, 45; b) C. Wen, T. Hasegawa, T. Kanbara, S. Kagaya, T. Yamamoto, *J. Photochem. Photobiol. A: Chem.* **2000**, *133*, 59; c) K. Hasegawa, C. Wen, T. Kotani, T. Kanbara, S. Kagaya, T. Yamamoto, *J. Mater. Sci. Lett.* **1999**, *18*, 1091; d) G. Cik, M. Hubinova, F. Sersen, J. Kristin, M. Antosova, *Collect. Czech. Chem. C* **2003**, *68*, 2219; e) G. Cik, F. Sersen, A. Bumbalova, *Collect. Czech. Chem. C* **1999**, *64*, 149; f) B. Muktha, G. Madras, T. N. G. Row, U. Scherf, S. Patil, *J. Phys. Chem. B* **2007**, *111*, 7994.
- [17] a) S. Yanagida, M. Hanazawa, A. Kabumoto, C. Pac, *Synth. Met.* **1987**, *18*, 785; b) M. Maruo, K. Yamada, Y. Wada, S. Yanagida, *Bull. Chem. Soc. Jpn.* **1993**, *66*, 1053; c) T. Ogata, K. Hiranaga, S. Matsuoka, Y. Wada, S. Yanagida, *Chem. Lett.* **1993**, *22*, 983; d) S. Yanagida, A. Kabumoto, K. Mizumoto, C. Pac, K. Yoshino, *J. Chem. Soc., Chem. Commun.* **1985**, 474; e) S. Matsuoka, H. Fujii, C. Pac, S. Yanagida, *Chem. Lett.* **1990**, 1501; f) S. Matsuoka, T. Kohzuki, A. Nakamura, C. Pac, S. Yanagida, *J. Chem. Soc., Chem. Commun.* **1991**, 580; g) S. Matsuoka, K. Yamamoto, C. Pac, S. Yanagida, *Chem. Lett.* **1991**, 2099; h) S. Yanagida, S. Matsuoka, *SPIE Proceeding Ser.* **1992**, *1729*, 243; i) S. Matsuoka, T. Kohzuki, T. Kuwana, A. Nakamura, S. Yanagida, *J. Chem. Soc. Perkin Trans. 2* **1992**, 679; j) S. Matsuoka, K. Yamamoto, T. Ogata, M. Kusaba, N. Nakashima, E. Fujita, S. Yanagida, *J. Am. Chem. Soc.* **1993**, *115*, 601; k) T. Ogata, S. Yanagida, B. S. Brunschwig, E. Fujita, *J. Am. Chem. Soc.* **1995**, *117*, 6708; l) T. Ogata, Y. Yamamoto, Y. Wada, K. Murakoshi, M. Kusaba, N. Nakashima, A. Ishida, S. Takamuku, S. Yanagida, *J. Phys. Chem.* **1995**, *99*, 11916; m) Y. Wada, T. Ogata, K. Hiranaga, H. Yasuda, T. Kitamura, K. Murakoshi, S. Yanagida, *J. Chem. Soc. Perkin Trans. 2* **1998**, 1999; n) Y. Wada, T. Kitamura, S. Yanagida, *Res. Chem. Intermed.* **2000**, *26*, 153; o) K. Maruo, K. Yamada, Y. Wada, S. Yanagida, *Bull. Chem. Soc. Jpn.* **1993**, *66*, 1053.
- [18] T. Yamamoto, A. Yamamoto, *Chem. Lett.* **1977**, *6*, 353.
- [19] S. Matsuoka, H. Fujii, T. Yamada, C. Pac, A. Ishida, S. Takamuku, M. Kusaba, N. Nakashima, S. Yanagida, *J. Phys. Chem.* **1991**, *95*, 5802.
- [20] a) M. Newcomb in *Reactive Intermediate Chemistry*, 1st ed. (Eds.: R. A. Moss, M. S. Platz, M. Jones), John Wiley & Sons, Hoboken, NJ, **2005**, vol. 1, p. 121; b) L. Routaboul, N. Vanthuyne, S. Gastaldi, G. Gil, M. Bertrand, *J. Org. Chem.* **2008**, *73*, 364; c) Y. Riyad, R. Hermann, O. Brede, *Radiat. Phys. Chem.* **2005**, *72*, 437.
- [21] a) M. M. Kreevoy, E. T. Harper, R. E. Duvall, H. S. Wilgus III, L. T. Ditsch, *J. Am. Chem. Soc.* **1960**, *82*, 4899; b) J. Tileston, J. Wymann, *Biophysical Chemistry*, Academic Press, Inc., New York, **1958**, vol. 1.
- [22] L. Ferry, W. H. Glaze, *J. Phys. Chem. B* **1998**, *102*, 2239.
- [23] K. E. O'Shea, S. Beightol, I. Garcia, M. Aguilar, D. V. Kalen, W. J. Cooper, *J. Photochem. Photobiol. A: Chem.* **1997**, *107*, 221.
- [24] S. L. Murov, I. Carmichael, G. L. Hug, *Handbook of Photochemistry*, 2nd ed., Marcel Dekker, New York, NY, **1993**.
- [25] N. S. Lewis, *Acc. Chem. Res.* **1990**, *23*, 176.
- [26] M. Nakamura, O. Ito, M. Matsuda, *J. Am. Chem. Soc.* **1980**, *102*, 698.
- [27] E. Hayon, M. Simic, *Acc. Chem. Res.* **1974**, *7*, 114.
- [28] A. Fattahi, S. R. Kass, *J. Org. Chem.* **2004**, *69*, 9176.
- [29] J. Broomhead, F. P. Dwyer, *Aust. J. Chem.* **1961**, *14*, 250.
- [30] T. Yamamoto, Y. Hayashi, A. Yamamoto, *Bull. Chem. Soc. Jpn.* **1978**, *51*, 2091.
- [31] W. Zhang, C. Li, *J. Chem. Soc. Perkin Trans. 1* **1998**, 3131.

Received: April 4, 2012

Published Online: ■

## Visible-Light Photocatalysis

Visible-light irradiation of poly(*p*-phenylene) in the presence of a sacrificial electron donor catalyzed the one-electron reduction of aryl aldehydes to generate ketyl intermediates. The ketyl intermediates undergo pinacol coupling reactions, and in the presence of thiol hydrogen atom donors, they can be diverted into a formal photoreduction to form alcohols.

**M. Zhang, W. D. Rouch,****R. D. McCulla\*** ..... 1–11

Conjugated Polymers as Photoredox Catalysts: Visible-Light-Driven Reduction of Aryl Aldehydes by Poly(*p*-phenylene)



**Keywords:** Photocatalysis / Conjugation / Polymers / Chemoselectivity / Reduction